Technical Note
Vadose Zone Journal

Estimation of Soil Water Balance Components Using an Iterative Procedure

R. C. Schwartz,* R. L. Baumhardt, and T. A. Howell

Quantifying the hydrologic balance at high temporal resolution is necessary to evaluate field-scale management effects on soil water storage. Our objective was to develop and evaluate a hybrid procedure to estimate drainage, infiltration, and evaporation based on changes in plot-scale soil water storage on a Pullman clay loam. Soil water contents were monitored in 2005 at 0.5-h intervals on 12 plots instrumented with time-domain reflectometry probes at 0.05, 0.1, 0.15, 0.2, and 0.3 m depths, and weekly using a neutron moisture meter to a depth of 2.3 m in 0.2-m increments. During periods in August 2005 when either a plane of zero flux existed or when a wetting front penetrated into an upper soil layer at ~0.24 m, changes in soil water storage were used to iteratively fit hydraulic parameters to estimate soil water fluxes into and out of the control volume. Predicted hydraulic conductivities were not significantly different (p = 0.471) from hydraulic conductivities calculated using the iterative method during three other months in 2005 and yielded drainage rates that differed by less than 0.05 mm d^{-1} as compared to calculated changes in storage below the plane of zero flux. By considering the delayed response of water content measurements to precipitation inputs, cumulative infiltration and evaporation throughout a month with 103-mm precipitation could be estimated from the measured changes in soil water storage with expected uncertainties of ± 5 mm. The proposed procedure permits the indirect estimation of soil water balance components useful for comparing plot-scale treatments and overcomes some of the difficulties associated with weighing lysimeter and meterological approaches.

Abbreviations: DOY, day of year; ET, evapotranspiration; ST, sweep tillage; TDR, time-domain reflectometry; UT, untilled; VGM, van Genuchten–Mualem.

Quantification of the hydrologic balance at high temporal resolution under field- or plot-scale conditions is necessary for evaluating management effects on infiltration and soil water storage. Meteorological methods are typically not suitable for small field- or plot-scale studies, whereas weighing lysimeters may restrict or compromise the application of large-scale treatments such as tillage. When carefully completed, an analysis of the change in soil water storage can provide accurate estimates of soil water conductivity at the lower boundary and, in this manner, enable the determination of water balance and crop water use throughout a season (Rose, 1966).With the development of automated soil water content measurements afforded by time-domain reflectometry (TDR) coupled with progress in waveform interpretation in natural field soils, accurate measurement of field soil water contents at high temporal resolution has recently become attainable. High-frequency sampling of soil water contents within the profile has the potential to accurately resolve the hydrologic balance within a control volume, provided it is coupled with estimates of drainage and runoff (Young et al., 1997).

The plane of zero flux method can be used to estimate drainage from a control volume within the soil profile. This method requires the measurement of soil water contents throughout the profile and the delineation of a plane where the total soil water potential gradient is zero. Net soil water flux is assumed to be in an upward direction above this plane and downward below it. The concept of the existence of a zero flux or "static" zone was first introduced by Richards et al. (1956), used by Jackson et al. (1973) to calculate diel soil water fluxes near the surface of a bare soil, and later refined by Arya et al. (1975) and Olsson and Rose (1978) to assess conductivities at any number of soil depths. When plant roots are restricted to depths above the plane of zero flux, drainage can be estimated by determining the change in soil water content below this plane. During periods with no rainfall, evapotranspiration can also be estimated by determining the change in soil water content above the plane. Unfortunately, this method often fails during periods after significant precipitation events where the hydraulic gradient becomes positive downward throughout the profile. Moreover, the depths of the zero flux planes are never stationary and can be difficult to determine when plants are actively transpiring (Arya, 2002). Despite these difficulties, an advantage of this method is that hydraulic conductivities can be estimated in situ.

Rose et al. (1965) developed a general method to determine the hydraulic conductivity of unsaturated field soils by

USDA-ARS, Conservation and Production Research Lab., P.O. Drawer 10, Bushland, TX 79012. The mention of trade or manufacturer names is made for information only and does not imply an endorsement, recommendation, or exclusion by USDA-ARS. Received 11 Jan. 2007. *Corresponding author (rschwartz@cprl.ars.usda.gov).

Vadose Zone J. 7:115–123
doi:10.2136/vzj2007.0006

© Soil Science Society of America
677 S. Segoe Rd. Madison, WI 53711 USA.
All rights reserved. No part of this periodical may be reproduced or transmitted in any form or by any means, electronic or mechanical, including photocopying, recording, or any information storage and retrieval system, without permission in writing from the publisher.

successive measurements of water content profiles and potential gradients inferred using soil water characteristics. Correction of the unloaded soil water characteristics resulting from the effects of overburden, however, was necessary to infer soil water potentials within the profile. In addition, Rose et al. (1965) applied an upper-boundary flux equivalent to the potential evaporation rate or some fraction thereof to enable the calculation of drainage rates within the profile. In contrast to Rose et al. (1965), Arya et al. (1975) inferred soil water contents from measured soil water potentials using tensiometers and laboratory-measured soil water characteristic relationships. Construction of water potential gradients with depth permitted the delineation of the plane of zero flux, although overburden effects were not considered when converting pressure heads to soil water contents (Arya et al., 1975). Olsson and Rose (1978) improved the general method proposed by Rose et al. (1965) by measuring both water contents and soil water potential directly to permit the determination of the plane of zero flux and thence drainage rates throughout the profile.

An alternative approach for estimating drainage is based on Darcy's equation. Soil water flux deep in the profile is estimated as the product of the water potential gradient and unsaturated conductivity. Typically, hydraulic conductivities are estimated on the basis of permeability tests performed on extracted soil cores. However, an accurate and representative determination of hydraulic conductivities from extracted soil cores is problematic principally because it may not adequately represent plot and field-scale processes (Beven, 1989).

The objective of this study is to introduce a hybrid method to determine soil water drainage for a bare soil based on the implementation of an iterative plane of zero flux method at selected time periods. As did Rose et al. (1965), we infer soil water potentials from measured soil water contents. In this study, however, effective plot scale parameters of hydraulic functions are optimized using field data to evaluate potential gradients and fluxes. Subsequently, fitted hydraulic parameters are used to estimate drainage based on the direct approach with Darcy's equation to calculate evaporation during time periods without precipitation. We also introduce a procedure to partition surface flux into infiltration and evaporation during precipitation events.

Theory

Consider a time series of soil water contents $\theta(z, t)$ ($m^3\ m^{-3}$) that are measured at equal and short time intervals ($\Delta t \leq 1$ h) and at depth increments small enough to permit the evaluation of the gradient near the surface($\Delta z \leq 0.1$ m). We seek a solution to the hydrologic balance of water within a control volume with an nonvegetated surface such that

$$S(t) - S(t - \Delta t) = D(Z, t) + I(t) + E(t) \qquad [1]$$

where $D(Z,t)$, $I(t)$, and $E(t)$ are depths (mm) of drainage, infiltration, and evaporation occurring in the time interval $t - \Delta t$. Here we adopt the convention that fluxes into a control volume are positive and fluxes out of the control volume are negative, irrespective of the flow direction. $S(t)$ is the area averaged volume of soil water (mm) stored at time t in a control volume extending from the surface to a constant lower boundary depth Z:

$$S(t) = \int_0^Z \theta(z, t)\mathrm{d}z \qquad [2]$$

where z is soil depth taken positive downward. Likewise, $S_L(t)$ is the volume of water stored at time t below a plane of zero flux $z_0(t)$ is

$$S_L(t) = \int_{z_0(t)}^Z \theta(z, t)\mathrm{d}z \qquad [3]$$

Here, $z_0(t)$ is approximated from the local maximum of the cubic spline interpolant of total soil water potential $H(z,t) = h(z, t) - z$. For this analysis, we assume that soil water potential $h(z, t)$ can be described by a soil water characteristic function $\theta(h)$ representative of an approximately homogenous soil horizon or profile extending from the minimum attained value of $z_0(t)$ to Z.

Let $\chi_{i,j}$ represent two vectors describing two distinct time period classes, each with length $i = 1 \ldots N_j$ for which measured soil water contents are available. We define $\chi_{i,1}$ as the $j = 1$ vector of time periods in which a near stationary, well-defined plane of zero flux exists in conjunction with drainage at the lower boundary (i.e., $\Delta S_L(t) < 0$) under near-steady state conditions such that $\partial\theta(Z)/\partial t \approx 0$ and $\partial^2 S_L(t)/\partial t^2 \approx 0$. Assuming one-dimensional flow and no plant water uptake, flux density at $z = Z$ for the time period $\chi_{i,1}$ can be derived from the continuity equation as

$$q(Z, \chi_{i,1}) = \frac{\partial S_L(t)}{\partial t} \qquad t \in \chi_{i,1} \qquad [4]$$

Concomitant with the flux during time period $\chi_{i,1}$ is the upper boundary z_0, water content, and potential gradient, which are approximated as

$$\begin{aligned} z_0(\chi_{i,1}) &= \frac{1}{M}\sum_{k=1}^{M} z_0(t_k) \\ \theta(Z, \chi_{i,1}) &= \frac{1}{M}\sum_{k=1}^{M} \theta(Z, t_k) \qquad t_k \in \chi_{i,1} \\ \frac{\partial H(Z, \chi_{i,1})}{\partial z} &= \frac{1}{M}\sum_{k=1}^{M} \frac{\partial H(Z, t_k)}{\partial z} \end{aligned} \qquad [5]$$

where M is the number of data points measured for the particular time period, and the pressure potential $h(Z,\chi_{i,1})$ is estimated from $\theta(Z,\chi_{i,1})$ using a water characteristic function. In this manner, drainage flux can be estimated for several time periods over a range of soil water contents and potential gradients at the lower boundary. Note that it is not necessary for z_0 to be constant among all time periods but only approximately constant (e.g., $\Delta z_0 < 0.01$ m) within a time period.

In semiarid regions, the range in soil water contents at the lower boundary may be restricted to much less than saturation, thereby limiting the predictability of drainage flux to low rates. This restriction can be avoided in part by evaluating fluxes into the soil during or immediately after significant precipitation events. Let $\chi_{i,2}$ represent the second vector with N_2 time periods when $\Delta S_L(t) \gg 0$ and when the wetting front has not penetrated through the lower boundary (e.g., $\partial\theta(Z)/\partial t \approx 0$). Again, it is preferable to select periods where $\partial^2 S_L(t)/\partial t^2 \approx 0$ so that changes in storage over time are nearly linear. Estimation of z_0 is not required, and for convenience, we designate the upper boundary of the lower

layer z_c equivalent to $z_0(\chi_{1,1})$. Assuming homogeneity between Z and z_c and negligible hysteresis in the constitutive functions, a first approximation of flux density into the lower layer $q(z_c, \chi_{i,2})$ can be obtained by applying Darcy's Law to estimate $|D(Z, t)|$ and adding this result to the change in storage such that

$$\hat{q}(z_c, \chi_{i,2}) = \frac{\partial S_L(t)}{\partial t} - K[\theta(Z, \chi_{i,2})] \cdot \frac{\partial H(Z, \chi_{i,2})}{\partial z} \quad t \in \chi_{i,2} \qquad [6]$$

where $K(\theta)$ is hydraulic conductivity function with parameters that have yet to be optimized. Concomitant with the flux during time period $\chi_{i,2}$ are the water contents and potential gradients at both boundaries that are approximated as

$$\theta(z_c, \chi_{i,2}) = \frac{1}{M}\sum_{k=1}^{M}\theta(z_c, t_k)$$
$$\frac{\partial H(z_c, \chi_{i,2})}{\partial z} = \frac{1}{M}\sum_{k=1}^{M}\frac{\partial H(z_c, t_k)}{\partial z} \qquad t_k \in \chi_{i,2} \qquad [7]$$

$$\theta(Z, \chi_{i,2}) = \frac{1}{M}\sum_{k=1}^{M}\theta(Z, t_k)$$
$$\frac{\partial H(Z, \chi_{i,2})}{\partial z} = \frac{1}{M}\sum_{k=1}^{M}\frac{\partial H(Z, t_k)}{\partial z} \qquad t_k \in \chi_{i,2} \qquad [8]$$

where the pressure potential is inferred from measured soil water contents and the water characteristic function.

Because the $K(\theta)$ is unknown in Eq. [6], an iterative procedure is required to estimate fluxes into and out of the control volume. The parameters of the constitutive relationships $K(\theta)$ and $h(\theta)$ can be estimated by minimizing the sum of squared errors between the calculated water balance flux and the estimated Darcy flux using the weighted objective function

$$\mathbf{\Phi}(\boldsymbol{\beta}, \boldsymbol{\chi}) = \frac{1}{N_1}\sum_{i=1}^{N_1}\left(\ln\left[q(Z, \chi_{i,1})\right] - \ln\left\{\frac{\partial H(Z, \chi_{i,1})}{\partial z} \cdot K[\theta(Z, \chi_{i,1})]\right\}\right)^2 + \frac{1}{N_2}\sum_{i=1}^{N_2}\left(\ln\left[\hat{q}(z_c, \chi_{i,2})\right] - \ln\left\{\frac{\partial H(z_c, \chi_{i,2})}{\partial z} K[\theta(z_c, \chi_{i,2})]\right\}\right)^2 \qquad [9]$$

where $\boldsymbol{\beta}$ is the vector of optimized parameters that describe $K(\theta)$. For each trial solution for the current estimate of $\boldsymbol{\beta}$, soil water potentials, potential gradients, and predicted fluxes at both boundaries are recalculated (Fig. 1). Here we assume that a natural log transformation will stabilize the heterogeneous variance in flux estimates at low and high water contents. Minimization of the objective function can be implemented using any of the commonly available nonlinear, least-squares parameter optimization algorithms. Once the parameters of the hydraulic conductivity and water characteristic functions have been fitted, then drainage can approximated for time increment Δt as

$$D(Z, t) = K[\theta(Z, t)] \cdot \frac{\partial H(Z, t)}{\partial z} \cdot \Delta t \qquad [10]$$

and the net loss or gain of soil water at the surface boundary for time increment Δt becomes

$$F(0, t) = S(t) - S(t - \Delta t) - D(Z, t) \qquad [11]$$

Because soil water content measurements are subject to random errors, it is useful to apply a smoothing filter to permit the detection of significant trends in the data. We apply a Savitzky-Golay filter (Press et al., 1992) to replace the surface boundary flux $F(0,t)/\Delta t$ with a mass-conserving, smoothed flux $G(0,t)/\Delta t$.

Let $P(t)$ be the precipitation depth occurring within the time interval $t - \Delta t$. During periods of precipitation, a positive $G(0,t)$ signifying a net increase in soil water storage should be attributed to infiltration. Accordingly, infiltration depth within the time interval $t - \Delta t$ can be approximated as

$$I(t) = \begin{cases} G(0,t) \text{ if } \sum_{i=t-\tau}^{t} P(i) > \varepsilon \text{ and } \left[G(0,t) > 0 \text{ or } P(t) > \varepsilon\right] \\ 0 \text{ otherwise} \end{cases} \qquad [12]$$

where ε is the detection limit of the rain gage (e.g., a single tip) and τ is the time lag between infiltration and measurable increases in soil water content caused by retention storage and a time delay between infiltration and arrival of the wetting front within the measurement volume of the shallowest TDR probe. To reduce bias from estimates of infiltration, we assume evaporation does not occur during precipitation so that $I(t)$ may be set equivalent to $G(0,t)$ even when negative. Conversely, evaporation depth within the time interval $t - \Delta t$ can be approximated as

$$E(t) = \begin{cases} G(0,t) \text{ if } I(t) = 0 \\ 0 \text{ otherwise} \end{cases} \qquad [13]$$

Inspection of Eq. [1], [11], [12], and [13] demonstrates that soil water balance is preserved within the control volume. For time

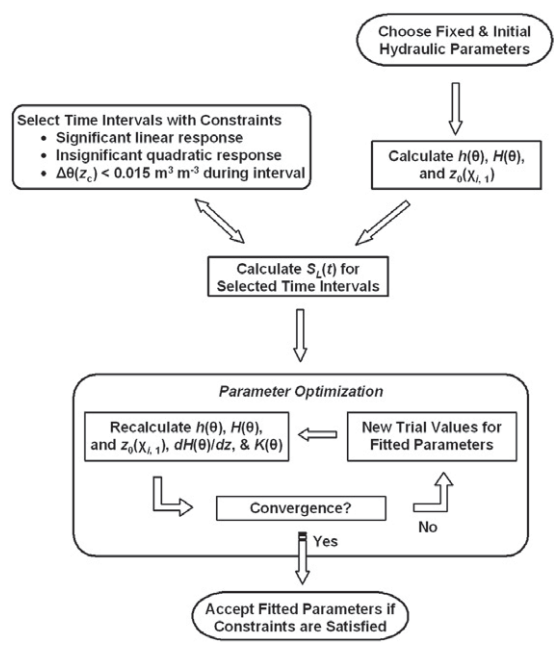

Fig. 1. Flowchart detailing the parameter optimization procedure for estimating hydraulic conductivity $K(\theta)$ using the change in soil water storage $S_L(t)$. Here, θ is soil water content, h is soil water potential, H is the total soil water potential, $z_0(\chi_{i,1})$ is the plane of zero flux at the ith time interval and $z_c = z_0(\chi_{i,1})$ at the $i = 1$ time interval.

periods with no precipitation, evaporation can be estimated with errors determined solely by the accuracy with which drainage flux can be predicted in Eq. [10] and the ability of the TDR array to resolve changes in soil water storage. During precipitation events, this accuracy is compromised, which poses a degree of uncertainty in estimated evaporation and runoff during these periods. Nonetheless, total soil water balance Eq. [1] is still valid because errors in estimating runoff and evaporation cancel out.

Materials and Methods

Field plots in Bushland, TX, were established in a fallow field under stubble-mulch tillage management on a Pullman clay loam (fine, mixed, superactive, thermic Torrertic Paleustolls). Clay contents and bulk densities of the Bt horizon were approximately uniform with respect to depth and tillage (Table 1). Plots were kept weed free and devoid of residue throughout the study period. In September 2004, the entire field was tilled using a para-plow to a depth of 0.3 m. Subsequently, thermocouples and 200-mm trifilar TDR probes were installed horizontally in 12 subplots at soil depths of 0.05, 0.1, 0.15, 0.2, and 0.3 m accessed through small (0.25 × 0.35 × 0.35 m) excavated pits. Waveforms were obtained using a cable tester (model 1502C, Tektronic, Inc., Beaverton, OR) and processed by a computer running the TACQ software (Evett, 2000a,b). Waveforms from each of the probes were acquired at half-hour intervals, and soil temperatures were recorded at 5-min intervals. Field water contents measured with TDR were estimated using square root of apparent permittivity calibrations (Ferré and Topp, 2002) with temperature compensation based on packed laboratory columns of Ap (0–0.15 m) and Bt (0.15–0.30 m) Pullman clay loam horizons.

Plots consisted of four parallel strips with alternating tillage treatments that were imposed in spring 2005. On 7 April, 20 May, and 21 July 2005, sweep-tillage (ST) strip plots were tilled to a depth of 0.07 to 0.1 m using a plow with two 0.9-m sweeps. The other two plots were untilled (UT) throughout the remainder of the year. Soil water contents were also monitored using a neutron moisture gage (model 503DR, Campbell Pacific Nuclear Int., Martinez, CA) at three locations in each of the four plots from 0.1 to 2.3 m depth in 0.2-m increments at weekly intervals. The gage was previously calibrated in situ on the Pullman soil at Bushland, TX. Ambient air temperature, relative humidity, wind velocity, net radiation (REBS Q7.1) at 1 m above tilled and untilled plots, and global irradiance (LICOR 200 pyronometer at 2 m) were also monitored during the study. Precipitation depth was recorded every 0.25 h with a tipping bucket rain gage.

Estimation of parameters using Eq. [9] was performed for soil water content data collected during August 2005 (see Fig. 1). The lower boundary depth Z was set to 0.6 m, which is within the clay-textured, noncalcareous Bt horizon (0.15–0.8 m). Besides TDR-measured water contents (0.05–0.3 m), we also used weekly measured neutron gage soil water contents at 0.5 and 0.7 m to permit integration of water contents to Z. Water content at $Z = 0.6$ m was estimated by averaging water contents measured at 0.5 and 0.7 m. The neutron gage-measured water contents were interpolated at 0.5-h intervals throughout the month to allow short-term water balance calculations. This was possible for these plots because average water contents at 0.5 and 0.7 m varied by no more than 0.003 $m^3\ m^{-3}$ during the month of August 2005. Water contents were averaged by depth across the six subplots to calculate changes in soil water storage with time for each tillage treatment. Average soil water contents were integrated with depth using the trapezoidal method and assuming that surface water content was equivalent to the water content measured at 0.05 m.

Constraints were imposed in the selection of time periods used in the determination of fluxes. Time periods were considered only if there was a significant ($p < 0.01$) slope response and a nonsignificant ($p > 0.01$) quadratic response to approximately satisfy steady state flux conditions. If a quadratic response was found significant, then the time period was shortened incrementally until the quadratic response was no longer significant. An additional constraint was also imposed for selecting time periods associated with soil water storage increases ($\chi_{i,2}$). The length of these time periods was limited such that net change in water contents measured by TDR probes inserted at 0.3 m was less than 0.015 $m^3\ m^{-3}$, the error associated with TDR water content measurements. Hence, during this time period, the wetting front would not have penetrated past 0.3 m, and consequently, negligible changes in water content at $Z = 0.6$ m could be assumed.

The van Genuchten–Mualem (VGM) model (van Genuchten, 1980)

$$K(\theta) = K_s\, s^{\frac{1}{2}}\left[1-\left(1-s^{\frac{1}{m}}\right)^m\right]^2$$
$$\theta(h) = \theta_r + \frac{\theta_s-\theta_r}{\left(1+|\alpha h|^n\right)^m} \qquad [14]$$

was used to describe the constitutive soil hydraulic properties in the Bt horizon. Here, θ_r and θ_s are the residual and saturated water contents ($m^3\ m^{-3}$), respectively, K_s is the saturated hydraulic conductivity ($m\ d^{-1}$), s is the effective saturation $[\theta(h) - \theta_r]/(\theta_s - \theta_r)$, n and α (m^{-1}) are empirically fitted parameters, and $m = 1 - (1/n)$. For the minimization routine and corresponding drainage calculations, we set $\alpha = 23.3\ m^{-1}$ as obtained by Schwartz and Evett (2002) for the Pullman Bt horizon. Constraining α to a fixed value avoids nonuniqueness difficulties associated with fitting K_s and α simultaneously (Schwartz and Evett, 2002). The field saturated water content was set to 0.43 $m^3\ m^{-3}$ based on measured flattened peak water contents at 0.2 and 0.3 m in the experimental plots during a significant precipitation event in June 2005. (A peak in soil water content that exhibits a flat response with time is indicative that field saturation has been attained.) The parameters K_s, n, and θ_r were estimated by minimization of the objective function using soil water content data measured in both UT and ST plots during August

Table 1. Particle size distribution† and bulk density of the study site. Means followed by 95% confidence intervals. Number of observations = 4.

Tillage depth	Sweep-tilled plots			Untilled plots		
	Clay	Silt	Bulk density	Clay	Silt	Bulk density
m	%	%	Mg m^{-3}	%	%	Mg m^{-3}
0–0.15	47.9 ± 3.1	37.2 ± 5.1	1.40 ± 0.11	47.7 ± 2.1	36.1 ± 4.3	1.45 ± 0.06
0.15–0.3	50.2 ± 1.5	37.7 ± 1.9	1.41 ± 0.10	51.9 ± 1.6	34.3 ± 2.0	1.43 ± 0.11
0.3– 0.45	51.6 ± 1.8	36.5 ± 2.0	1.42 ± 0.12	52.2 ± 1.7	33.2 ± 5.6	1.45 ± 0.03
0.45–0.6	51.4 ± 2.9	37.5 ± 1.7	1.42 ± 0.03	50.7 ± 1.1	36.9 ± 2.9	1.41 ± 0.08
0.6–0.75	48.8 ± 2.6	36.0 ± 2.8	1.39 ± 0.09	49.2 ± 1.6	35.1 ± 2.8	1.37 ± 0.03

† Particle-size distribution determined using the hydrometer method (Gee and Bauder, 1986).

2005. Although tillage modified the surface horizon and hence infiltration rates, soil properties of the Bt horizon would be expected to be similar between treatments because tillage was limited to ~0.1 m. Final parameter estimates were determined by minimization of the objective function implemented with the Excel solver program which uses the generalized reduced gradient method (Lasdon et al., 1978) with forward differencing. Iterations of the nonlinear least-squares estimation procedure were continued until the maximum scaled relative change in the objective function was less than 0.0001. The residual water content was constrained to $\theta_r \leq 0.15$ m^3 m^{-3} to satisfy a minimum water content of ~0.18 m^3 m^{-3} recorded in the Bt horizon at this site planted to dryland grain sorghum [*Sorghum bicolor* (L.) Moench] in 2006.

Table 2. Fluxes, water contents, water potentials, and potential gradients associated with the optimized drainage solution for August 2005.†

Drainage at lower boundary (Eq. [4, 5])

Day of year	Field‡	z_0	$\partial S_L(t)/\partial t$§	$\theta(Z)$	$h(Z)$	$\partial H(Z)/\partial z$	$K[\theta(Z)]$
		m	mm d^{-1}	m^3 m^{-3}	m		mm d^{-1}
213–219	UT	0.238 (0.001)	−0.166 (0.024)	0.341 (<0.001)	−0.29	−1.57 (<0.01)	0.106
240–244	UT	0.228 (0.002)	−0.117 (0.035)	0.339 (<0.001)	−0.30	−1.57 (<0.01)	0.075
215–219	ST	0.236 (<0.001)	−0.133 (0.038)	0.337 (<0.001)	−0.33	−1.53 (0.01)	0.087
240–244	ST	0.235 (<0.001)	−0.083 (0.044)	0.342 (<0.001)	−0.28	−1.75 (0.01)	0.048

Drainage at upper boundary (Eq. [6, 7, 8])

Day of year	Field	z_c	$\partial S_L(t)/\partial t$	$K(\theta)\cdot\partial H(Z)/\partial z$	$\theta(z_c)$	$h(z_c)$	$\partial H(z_c)/\partial z$	$K[\theta(z_c)]$
		m	mm d^{-1}	mm d^{-1}	m^3 m^{-3}	m		mm d^{-1}
226.8–227.7	UT	0.238	1.45 (0.35)	−0.176	0.380 (0.003)	−0.09	−0.62 (0.09)	2.63
226.7–227.5	ST	0.236	3.31 (0.46)	−0.166	0.394 (0.005)	−0.06	−0.66 (0.06)	5.30

Optimization results¶

Parameter	Value	Lower 95% CI#	Upper 95% CI
n	1.193	1.171	1.223
K_s (mm d^{-1})	578.4	312.8	1072

† Values in parenthesis are ± 95% confidence intervals of the estimated linear regression slope for fluxes and ± mean standard deviations for all other variables; $\partial S_L(t)/\partial t$ is the change in storage with time; $\theta(Z)$ is the mean water content at $z = Z$; $h(Z)$ is the corresponding pressure head; $\partial H(Z)/\partial z$ is the mean total potential gradient; $K[\theta(Z)]$ is the fitted hydraulic conductivity at $z = Z$; $K(\theta)\cdot\partial H(Z)/\partial z$ is the Darcy flux velocity at $z = Z$; z_0 is the mean plane of zero flux; and z_c is equivalent to z_0 obtained for the first drainage time period.

‡ UT, untilled plots; ST, sweep-tilled plots.

§ Positive changes in storage $\partial S_L(t)/\partial t$ signify net flow into the control volume and negative changes signify flow out of the control volume.

¶ Optimized results based on August 2005 data. Fixed parameters are $\theta_s = 0.43$ m^3 m^{-3}, $\theta_r = 0.15$ m^3 m^{-3}, and $\alpha = 23.3$ m^{-1}.

Lower and upper 95% confidence intervals (CI) are calculated using the generalized likelihood ratio test (Lehmann, 1986).

The total soil water potential gradient at 0.6 m was estimated by a first order approximation using calculated $h(\theta)$ at 0.5 and 0.7 m. A cubic spline interpolation of H from 0.15 to 0.5 m, with the second derivative set equivalent to zero at the end knots, was used to estimate z_0 and $\partial H(z_c)/\partial z$. The change in storage $\partial S_L(t)/\partial t$ was determined by finding the slope of soil water storage curve with time for each respective period χ. Smoothing of $F(0,t)$ was performed using a Savitzky–Golay filter of degree four (Press et al., 1992). A moving window of nine data points was chosen to preserve the width of the infiltration events to within plus or minus one time interval of the width indicated by positive changes in storage during precipitation events in the month of August. In Eq. [12], ε was set to 0.1 mm and τ was set to 0.0833 d. Reference evapotranspiration (ET_0) was determined with the ASCE equations (Allen et al., 2005) for a short grass reference crop using meteorological data collected at the site. Net radiation was calculated as a function of global irradiance using the equations presented by Allen et al. (2005).

Results and Discussion

Three time periods in August 2005 were chosen for each tillage treatment to estimate drainage using the plane of zero flux method (Table 2). All selected periods exhibited linear ($p < 0.01$) changes in $S_L(t)$ with time (Fig. 2), resulting in estimated fluxes with 95% confidence limits less than ± 0.05 and ± 0.46 mm d^{-1} for drainage at the lower and upper boundary, respectively (Table 2). Changes in z_0 during selected drainage time periods were less than 0.01 m. Deviations in z_0, $\theta(Z)$, $\theta(z_c)$, $\partial H(Z)/\partial z$, and $\partial H(z_c)/\partial z$ were likewise small within all time periods (Table 2), which satisfies the assumptions for application of Eq. [4] and [6]. Minimization of the objective function resulted in θ_r increasing to the maximum bounded value (0.15 m^3 m^{-3}). With θ_r fixed at 0.15 m^3 m^{-3}, the $K_s - n$ response surface exhibited a well-defined minima (Fig. 3) with narrow confidence limits for n and larger confidence limits for K_s (Table 2). Šimůnek and van Genuchten (1996) and Schwartz and Evett (2002) presented similarly shaped response surfaces for objective functions where both cumulative infiltration and water contents were measured. Parameter optimization based on the water contents measured in August (Table 2 and Fig. 4) yielded a value of $n = 1.19$, typical of clays and silty clays (Yates et al., 1992), although the predicted VGM retention function underestimated water contents compared with the retention data obtained from Pullman soil cores in the Bt horizon

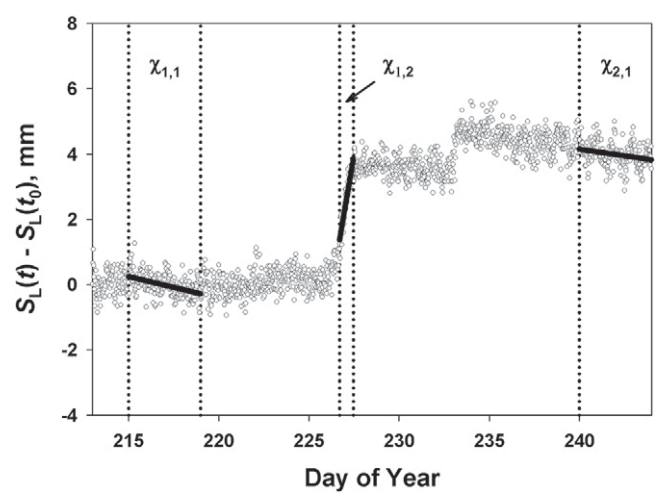

Fig. 2. Change in soil water storage with time $S_L(t)$ for the sweep-tilled (ST) plots and the associated time period classes for drainage at the lower boundary ($\chi_{1,1}$ and $\chi_{2,1}$) and into the upper boundary ($\chi_{1,2}$). Solid lines are fitted fluxes for each time period. Each point represents the average soil water storage for six profiles from z_c = 0.236 m to z = 0.6 m.

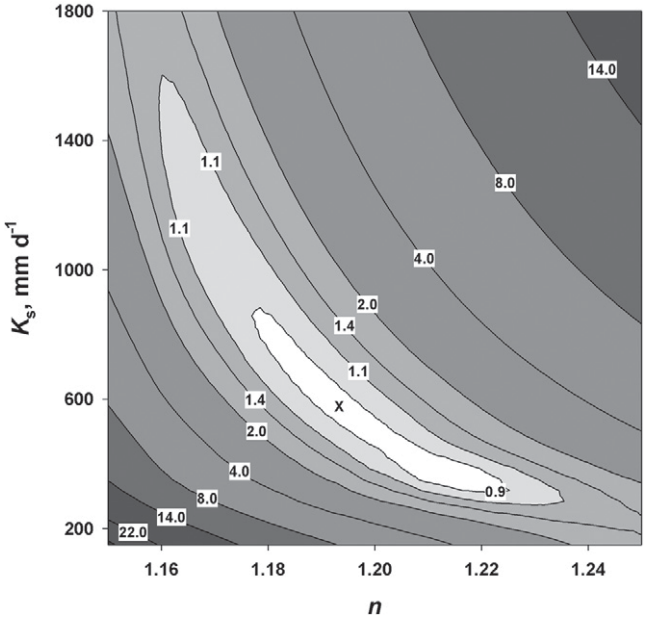

Fig. 3. Response surface of the objective function in the n–K_s parameter plane. The location of the optimized solution is marked with an "X." K_s = saturated hydraulic conductivity; n = empirically fitted parameter.

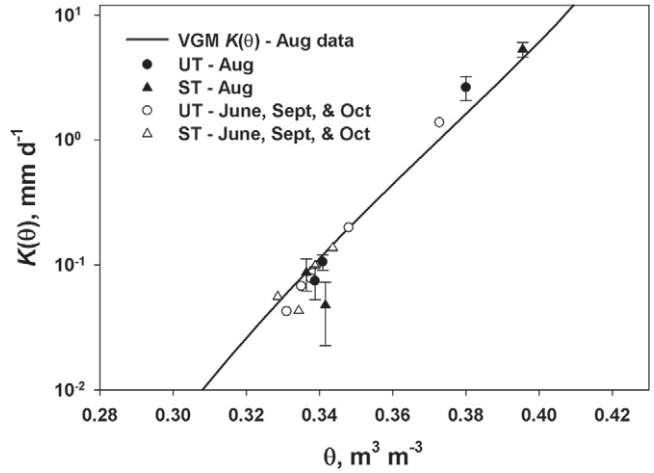

Fig. 4. Optimized hydraulic conductivity relationship $K(\theta)$ based on August, 2005 data and the corresponding measured conductivities in August (filled symbols) and June, September and October (unfilled symbols). Parameter optimization results are shown in Table 2. Error bars are 95% confidence limits of fluxes divided by hydraulic gradients. θ = water content; VGM = van Genuchten–Mualem model; UT = untilled plots; ST = sweep-tilled plots.

(Schwartz and Evett, 2002). The tendency for laboratory measured soil water contents to exceed field-measured values at water potentials near saturation is characteristic of fine-textured soils (Olsson and Rose, 1978; Pachepsky et al., 2001) and, for this study, may be a result of differences in measurement scale, heterogeneity within the Bt horizon (e.g., Green et al., 1996), overburden pressure, or dynamic nonequilibrium (Schultze et al., 1999; Ross and Smettem, 2000). Hence, the fitted results are effective parameters that reflect ensemble hydraulic responses of the Bt horizon at the plot or field scale (Kabat et al., 1997).

Maximum deviations about the fitted regression lines for $S_L(t)$ versus time were approximately ± 1 mm and the root mean square errors averaged ± 0.32 mm for the month of August 2005 (see Fig. 2). Accordingly, the precision with which changes in soil water can be measured for this field setup were approximately 0.32 and 0.6 mm for the lower and entire control volumes, respectively. Upon averaging and integration, random errors generated by waveform interpretation of the 30 TDR probes tended to cancel out and led to greater precision in estimating changes in soil water storage.

Drainage rates predicted using Eq. [10] with the fitted $K(\theta)$ function from August data differed by less than 0.05 mm d^{-1} compared with the change in storage below the plane of zero flux calculated for eight other selected time periods throughout 2005 (Fig. 5; October data not shown). Moreover, hydraulic conductivities based on estimated fluxes and potential gradients in June, September, and October were not significantly different (p = 0.471) from the fitted $K(\theta)$ function (Fig. 4). Closer examination of Fig. 5 after 107 mm of precipitation in early June illustrates that greater flux into the lower control volume of UT plots resulted in a steeper drainage curve with an additional ~2 mm of predicted drainage throughout the remainder of the month compared with the ST plots. Most of the additional drainage (~75%) for the UT plots occurred before DOY 172 when soil water contents and gradients were changing rapidly and a satisfactory and stable value of z_0 could not be discerned. In contrast to the traditional plane of zero flux method, drainage based on the fitted solution to $K(\theta)$ can be estimated throughout periods when z_0 does not exist. However, soil water contents at the lower boundary still need to be measured with sufficient frequency to detect the movement of wetting fronts through the profile. Otherwise, soil water fluxes may be underestimated.

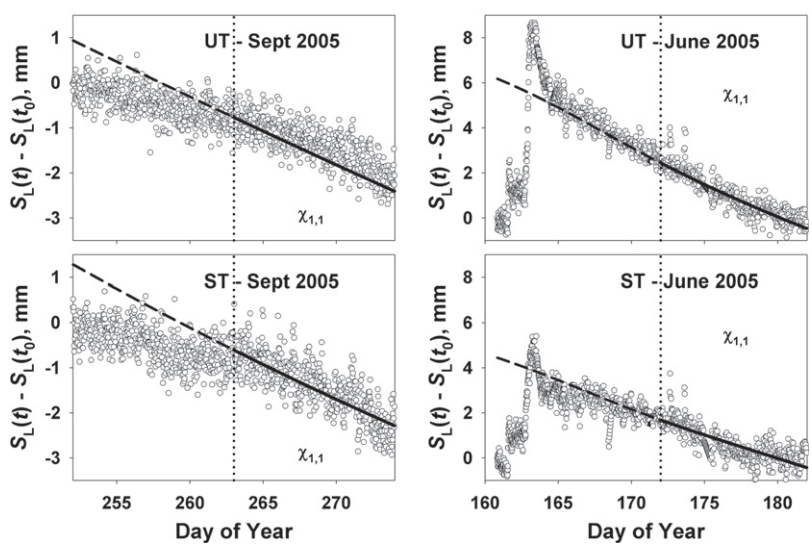

Fig. 5. Change in soil water storage with time, $S_L(t)$ for a dry month (September 2005) and wet month (June 2005), and corresponding predicted drainage at the lower boundary for periods when a well-defined plane of zero flux existed (solid line) and other periods (dashed line). Predicted cumulative drainage $D(Z, t_1)$ is offset at the beginning of each period t_1 such that $D(Z, t_1) = S_L(t_1) - S_L(t_0)$ where $S_L(t_1)$ and $S_L(t_0)$ are soil water storage at time t_1 and the initial time t_0, respectively.

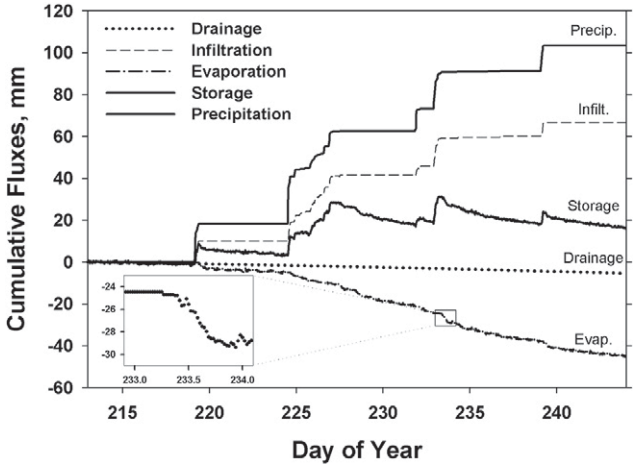

Fig. 6. Estimated soil water balance within the 0- to 0.6-m control volume for the sweep-tilled plots in month of August 2005. Inset graph is estimated evaporation during DOY 233.

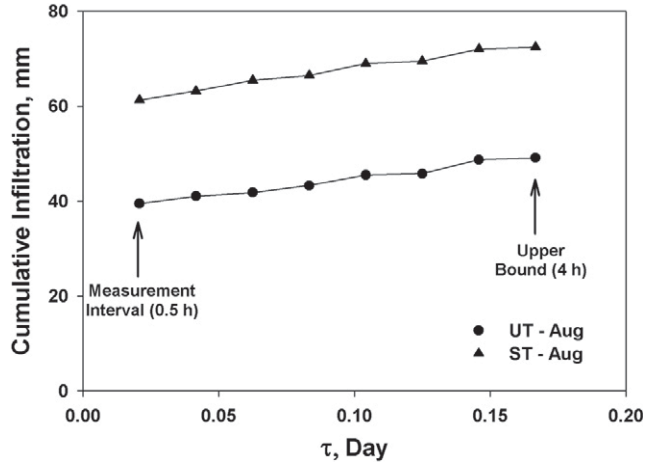

Fig. 7. Sensitivity of cumulative infiltration to the time lag τ during the month of August with 103 mm of precipitation. The upper bound on the time lag reflects the time required for infiltration of water ponded to a depth equivalent to the maximum depressional storage. UT = untilled plots; ST = sweep-tilled plots.

Once drainage is estimated at $z = Z$, components of the soil water balance can be partitioned using Eq. [11], [12], and [13] as shown in Fig. 6 for the month of August 2005. Cumulative drainage was clearly a small component of the water balance during this month and amounted to approximately 5.3 mm in each tillage treatment. Periods of infiltration corresponded closely with precipitation events and suggest approximately 64 and 42% of the cumulative precipitation infiltrated during this month for the ST and UT treatments, respectively. These fractions compare closely to those measured using a rotating disk rainfall simulator by Baumhardt and Jones (2002) on a Pullman soil in sweep and no-tillage fallow fields (68 and 46%, respectively). The error in cumulative infiltration resulting from the choice of the time lag τ can be estimated by considering the upper and lower bounds of τ. The minimum value of τ is the water content measurement interval (0.5 h) assuming negligible evaporation for this time period. For the plots in this study, we estimated an upper bound of τ = 4 h based on a maximum detention storage of 10 mm (Kamphorst et al., 2000) divided by a ponded steady-state surface infiltration rate of 2.5 mm h^{-1} for Pullman soils (Unger and Pringle, 1981). Cumulative precipitation that infiltrated was relatively insensitive to the time lag τ and ranged from 39 to 49 mm for UT plots and 61 to 72 mm for ST plots during August, with 103 mm of precipitation (Fig. 7). Cumulative evaporation exhibits precisely the same trend as precipitation due to the form of the expression in Eq. [13]. Accordingly, uncertainties in the estimated value of cumulative infiltration and evaporation in August for both plots are approximately ± 5 mm. This accuracy was considered sufficient for comparing differences between plot scale tillage treatments in August, which averaged 23 mm.

Without applying the Savitzky–Golay filter to the surface flux, sensitivity to τ doubled with a concomitant increase in the uncertainty to ± 10 mm of the estimated cumulative infiltration and evaporation in August. In addition, estimated infiltration increased by 14% (10 mm) during August in the ST plots with a concomitant increase in evaporation. Most of the increase in evaporation without the filter occurred in day of year (DOY) 225 and 226 with numerous precipitation events and led to suspect daily evaporation rates. The approach used to partition infiltration and evaporation is illustrated in detail for a single precipitation event in August 2005 (Fig. 8). Based on these soil water balance and precipitation data, application of the Savitzky-Golay filter reduced the level of noise and preserved the heights and widths of the peaks representing changes in storage caused by precipitation.

Estimated bare-soil evaporation for the ST plots fall within the range reported for fine textured soils under semiarid conditions (e.g., Wythers et al., 1999). Daily rates of bare-soil evaporation were less than or not significantly different (± 0.6 mm) from reference evapotranspiration (ET_0) in all but 2 d (227 and 233) during the month of August 2005 (Fig. 9). A significant precipitation event preceded both of these periods in which bare-soil evaporation exceeded ET_0 by approximately 1.6 mm. An underestimation of drainage does not explain the decreased stor-

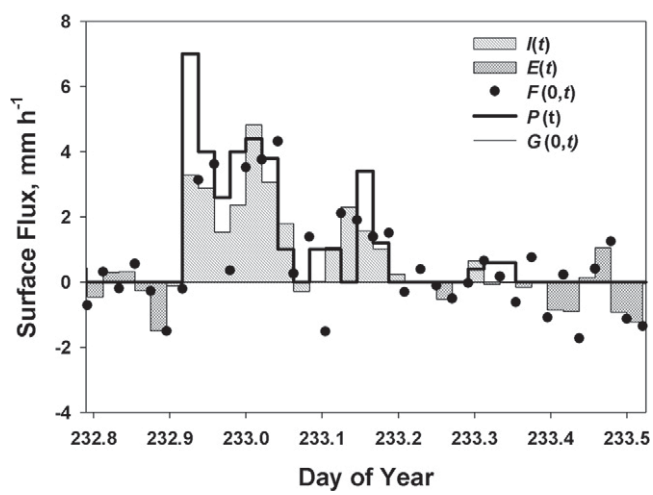

Fig. 8. Partitioning of infiltration $I(t)$ and evaporation $E(t)$ using Eq. [12] and [13] for the sweep-tilled plots during a low-intensity precipitation $P(t)$ event. $F(0,t)$ and $G(0,t)$ are the unfiltered and filtered fluxes, respectively, at the soil surface during the time increment $t - \Delta t$. Cumulative infiltration and evaporation totaled 13.1 and 2.5 mm, respectively, for this time period and are equivalent to the shaded area above the zero flux line less the shaded area below. Total precipitation during this time period was 17.5 mm.

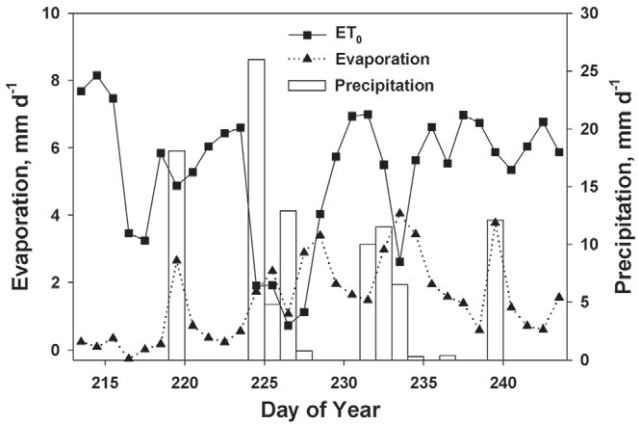

Fig. 9. Precipitation, estimated daily bare-soil evaporation and grass reference evapotranspiration (ET_0) for the sweep-tilled plots in August 2005.

age because nearly all of the soil water content changes occurred during the daytime for both days (see Fig. 6, inset). Likewise, decreasing the time lag τ had no effect on predicted evaporation because the preceding rainfall events were continuous. Both days are characterized by the greatest measured 0.05-m water contents throughout the month (0.20–0.37 $m^3\ m^{-3}$), low daily net radiation (4.35 and 9.07 MJ $m^{-2}\ d^{-1}$), moderate daytime vapor pressure deficits (maximum of 0.80 and 1.18 kPa), and moderate wind speeds (maximum of 2.9 and 5.8 m s^{-1}). Under these stable and transitional atmospheric conditions, sensible heat flux becomes negative and radiation-dominated ET models can underestimate potential evaporation from a wet bare-soil surface (Parlange and Katul, 1992).

Conclusions

A modified plane of zero flux procedure was proposed that iteratively fits $K(\theta)$ based on soil water content measurements integrated over space and time to calculate fluxes into and out of a control volume. Once the conductivity function is calibrated during suitable periods, drainage at the lower boundary of the control volume can be estimated directly as the product of the unsaturated conductivity and water potential gradient, both of which are estimated from measured water contents above and below the lower boundary. By evaluating fluxes into the lower control volume after significant precipitation events, the proposed method extended the range of water content values over which $K(\theta)$ could be calibrated. This method can be extended to greater soil depths with dissimilar hydraulic properties to estimate drainage below the root zone using the methods of Arya (2002). The difficulty herein lies in the restricted range of soil water contents that may occur in the soil horizon associated with the maximum rooting depth, which limits the range over which the hydraulic conductivity relationship can be fitted under a dryland cropping scenario. In such cases, irrigation of the field may be necessary to calibrate the hydraulic conductivity function. We recommend calibrating $K(\theta)$ under fallow conditions and applying these results to estimate drainage directly during the growing season. During periods of plant growth and root activity, a plane of zero flux may be difficult to discern because of increased spatial variability of soil water contents.

The strategies used to partition changes in soil water storage after accounting for drainage permitted us to estimate cumulative infiltration and evaporation with an upper and lower bounds of ± 5 mm throughout a month with 103 mm of precipitation. The expected uncertainties in these water balance components are a function of the sensitivity to the time lag chosen to reflect the delayed response of water content measurements to precipitation inputs. Large values of the time lag (e.g., 4 h) may result in erroneously attributing apparently random positive and negative changes in storage to infiltration and evaporation, respectively. Differentiating between real and random changes in storage to partition between these two balance components was most problematic during long, intermittent precipitation events.

While we acknowledge that the strategies used to partition infiltration and evaporation require further validation, the accuracy of estimated water balance components was sufficient to detect differences between plot-scale tillage treatments in this study. Moreover, calculated changes in total soil water balance are not influenced by these uncertainties. Hence, during periods with no precipitation, evaporation can be estimated with errors determined solely by the accuracy with which drainage flux is predicted and the resolution with which the TDR array can detect changes in soil water storage. These results suggest that soil water balance components calculated using the proposed procedure would useful for comparing plot-scale treatments that are difficult to evaluate using meteorological or weighing lysimeter techniques.

Acknowledgments

We gratefully acknowledge the technical assistance of Ms. Jourdan Bell for electronics, micrologger programming, and data compilation.

References

Allen, R.G., I.A. Walter, R.L. Elliot, and T.A. Howell (ed.). 2005. The ASCE standardized reference evapotranspiration equation. ASCE Press, Reston, VA.

Arya, L.M. 2002. Plane of zero flux. p. 945–953. *In* J. H. Dane and G. C. Topp (ed.) Methods of soil analysis: Part 4. Physical methods. SSSA, Madison, WI.

Arya, L.M., D.A. Farrell, and G.R. Blake. 1975. A field study of soil water depletion patterns in presence of growing soybean roots: I. Determination of hydraulic properties of the soil. Soil Sci. Soc. Am. Proc. 39:424–430.

Baumhardt, R.L., and O.R. Jones. 2002. Residue management and paratillage effects on some soil properties and rain infiltration. Soil Tillage Res. 65:19–27.

Beven, K. 1989. Changing ideas in hydrology: The case of physically-based models. J. Hydrol. 105:157–172.

Evett, S.R. 2000a. The TACQ program for automatic time domain reflectometry measurements: I. Design and operating characteristics. Trans. ASAE 43:1939–1946.

Evett, S.R. 2000b. The TACQ program for automatic time domain reflectometry measurements: II. Waveform interpretation methods. Trans. ASAE 43:1947–1956.

Ferré, P.A., and G.C. Topp. 2002. Time domain reflectometry. p. 434–446. *In* J. H. Dane and G. Clarke Topp (ed.) Methods of soil analysis. Part 4. Physical methods. SSSA, Madison, WI.

Gee, G.W., and J.W. Bauder. 1986. Particle-size analysis. p. 383–411. *In* A. Klute (ed.) Methods of soil analysis: Part 1. Physical and mineralogical methods. 2nd ed. SSSA, Madison, WI.

Green, T.R., J.E. Constantz, and D.L. Freyberg. 1996. Upscaled soil-water retention using van Genuchten's function. J. Hydrol. Eng. 1:123–130.

Jackson, R.D., B.A. Kimball, R.J. Reginato, and F.S. Nakayama. 1973. Diurnal soil-water evaporation: Time-depth-flux patterns. Soil Sci. Soc. Am. Proc. 37:505–509.

Kabat, P., R.W.A. Hutjes, and R.A. Feddes. 1997. The scaling characteristics of soil parameters: From plot scale heterogeneity to subgrid parameterization. J. Hydrol. 190:363–396.

Kamphorst, E.C., V. Jetten, J. Guérif, J. Pitkanen, B.V. Iversen, J.T. Douglas, and A. Paz. 2000. Predicting depressional storage from soil surface roughness. Soil Sci. Soc. Am. J. 64:1749–1758.

Lasdon, L.S., A.D. Waren, A. Jain, and M. Ratner. 1978. Design and testing of a generalized reduced gradient code for nonlinear programming. ACM Trans. Math. Softw. 4:34–50.

Lehmann, E.L. 1986. Testing statistical hypotheses (2nd ed.). John Wiley & Sons, New York.

Olsson, K.A., and C.W. Rose. 1978. Hydraulic properties of a red-brown earth determined from *in situ* measurements. Aust. J. Soil Res. 16:169–180.

Pachepsky, Y., W.J. Rawls, and D. Giménez. 2001. Comparison of soil water retention at field and laboratory scales. Soil Sci. Soc. Am. J. 65:460–462.

Parlange, M.B., and G.G. Katul. 1992. Estimation of the diurnal variation of potential evaporation from a wet bare soil surface. J. Hydrol. 132:71–89.

Press, W.H., S.A. Teukolsky, W.T. Vetterling, and B.P. Flannery. 1992. Numerical recipes in FORTRAN: The art of scientific computing. 2nd ed. Cambridge Univ. Press, New York.

Richards, L.A., W.R. Gardner, and G. Ogata. 1956. Physical processes determining water loss from soil. Soil Sci. Soc. Am. Proc. 20:310–314.

Rose, C.W. 1966. Agricultural physics. Pergamon Press, Oxford, UK.

Rose, C.W., W.R. Stern, and J.E. Drummond. 1965. Determination of hydraulic conductivity as a function of depth and water content for soil *in situ*. Aust. J. Soil Res. 3:1–9.

Ross, P.J., and K.R.J. Smettem. 2000. A simple treatment of physical nonequilibrium water flow in soils. Soil Sci. Soc. Am. J. 64:1926–1930.

Schultze, B., O. Ippisch, B. Huwe, and W. Durner. 1999. Dynamic nonequilibrium during unsaturated water flow. p. 877–892. *In* M.Th. van Genuchten et al. (ed.) Proc. Int. Workshop: Characterization and Measurement of the Hydraulic Properties of Unsaturated Porous Media, Riverside, CA. 22–24 Oct. 1997. Univ. of California, Riverside.

Schwartz, R.C., and S.R. Evett. 2002. Estimating hydraulic properties of a fine-textured soil using a disc infiltrometer. Soil Sci. Soc. Am. J. 66:1409–1423.

Šimůnek, J., and M.Th. van Genuchten. 1996. Estimating unsaturated soil hydraulic properties from tension disc infiltrometer data by numerical inversion. Water Resour. Res. 32:2683–2696.

Unger, P.W., and F.B. Pringle. 1981. Pullman soils: Distribution, importance, variability, and management. Texas Agric. Exp. Station, and USDA, Bushland, TX.

van Genuchten, M.Th. 1980. A closed-form equation for predicting the hydraulic conductivity of unsaturated soils. Soil Sci. Soc. Am. J. 44:892–898.

Wythers, K.R., W.K. Lauenroth, and J.M. Paruelo. 1999. Bare-soil evaporation under semiarid field conditions. Soil Sci. Soc. Am. J. 63:1341–1349.

Yates, S.R., M.Th. van Genuchten, and F.J. Leij. 1992. Analysis of predicted hydraulic conductivities using RETC. p. 273–282. *In* M.Th. van Genuchten et al (ed.) Indirect methods for estimating the hydraulic properties of unsaturated soils. U.S. Salinity Laboratory and Univ. of California, Riverside.

Young, M.H., P.J. Wierenga, and C.F. Mancino. 1997. Monitoring near-surface water storage in turfgrass using time domain reflectometry and weighing lysimetry. Soil Sci. Soc. Am. J. 61:1138–1146.